Advances in Applied Mathematics and Mechanics
Adv. Appl. Math. Mech., Vol. **xx**, No. x, pp. 1-25

DOI: 10.4208/aamm.OA-2023-0046
xxx 202x

Numerical Analysis of Stabilized Second Order Semi-Implicit Finite Element Methods for the Phase-Field Equations

Congying Li[1,*], Liang Tang[2] and Jie Zhou[3]

[1] *School of Mathematics and Computational Science, Huaihua University, Huaihua, Hunan 418000, China*
[2] *Key Laboratory of Intelligent Control Technology for Wuling-Mountain Ecological Agriculture in Hunan Province, School of Mathematics and Computational Science, Huaihua University, Huaihua, Hunan 418000, China*
[3] *School of Mathematics and Computational Science, Hunan Key Laboratory for Computation and Simulation in Science and Engineering, Xiangtan University, Xiangtan, Hunan 411105, China*

Received 9 February 2023; Accepted (in revised version) 16 June 2023

Abstract. In this paper, we consider two stabilized second-order semi-implicit finite element methods for solving the Allen-Cahn and Cahn-Hilliard equations. Stabilized semi-implicit schemes are used for temporal discretization, and the finite element method is used for spatial discretization. It is shown that by adding a single linear term that is of the same order with the truncation error in time, the proposed methods are all unconditionally energy stable. Error estimates for the two schemes are also established. Numerical examples are presented to confirm the accuracy, efficiency and stability of the proposed methods.

AMS subject classifications: 65N15, 65N30, 65M15

Key words: Allen-Cahn equation, Cahn-Hilliard equation, stabilized semi-implicit method, energy stable, error estimation.

1 Introduction

We consider in this work the numerical approximation of the Allen-Cahn equation

$$\begin{cases} \dfrac{\partial u}{\partial t} - \epsilon\Delta u + F'(u) = 0, & (x,t) \in \Omega \times (0,T], \\ u(x,0) = u_0(x), & x \in \Omega, \\ u(x,t) = 0, & (x,t) \in \partial\Omega \times (0,T], \end{cases} \tag{1.1}$$

*Corresponding author.
Emails: lcy1869@126.com (C. Li), 861316551@qq.com (L. Tang), zhouj@xtu.edu.cn (J. Zhou)

and the Cahn-Hilliard equation

$$\begin{cases} \dfrac{\partial u}{\partial t}+\Delta(\epsilon\Delta u-F'(u))=0, & (x,t)\in\Omega\times(0,T], \\ u(x,0)=u_0(x), & x\in\Omega, \\ \dfrac{\partial u}{\partial n}=\dfrac{\partial(\epsilon\Delta u-F'(u))}{\partial n}=0, & (x,t)\in\partial\Omega\times(0,T]. \end{cases} \tag{1.2}$$

Here $\Omega\subset R^d$ $d=(1,2,3)$ is a bounded domain, $\partial\Omega$ denotes the Lipschitz boundary of Ω. n denotes the unit outward normal vector of $\partial\Omega$. $T>0$ is a fixed constant. The parameter ϵ which models the effect of interfacial energy is small but always larger than zero. The Ginzburg-Landau double well potential $F(u)=(u^2-1)^2/4$ is considered, and the function $u(x,t)$ is a distribution function of the concentration for one of the two metallic components of the alloy. As we all know that the Allen-Cahn and Cahn-Hilliard equation can be regarded as the gradient flow of the following Liapunov energy functional

$$E(u)=\int_\Omega\Big(\frac{\epsilon}{2}|\nabla u|^2+F(u)\Big)dx \tag{1.3}$$

in L^2-space and H^{-1}-space, respectively. If we take the inner product for the first equation in (1.1) with u_t, we can obtain the following equality

$$(u_t,u_t)+\epsilon(\nabla u,\nabla u_t)+(u^3,u_t)-(u,u_t)=0,$$

and it is easy to show that for the the Allen-Cahn equation (1.1),

$$\frac{dE(u(t))}{dt}=\int_\Omega\epsilon\nabla u\nabla u_t+(u^3-u)u_t dx=-(u_t,u_t)\le 0. \tag{1.4}$$

Similarly, if we take the inner product for the first equation in (1.2) with $-\Delta^{-1}u_t$, we have

$$\|u_t\|_{-1}^2-(\nabla\mu,\nabla\mu)=0.$$

Here $\mu=\epsilon\Delta u-F'(u)$, and the H^{-1} norm $\|\cdot\|_{-1}$ is defined in the next section. Hence, we could prove that for the Cahn-Hilliard equation (1.2),

$$\frac{dE(u(t))}{dt}=\int_\Omega\epsilon\nabla u\nabla u_t+(u^3-u)u_t dx=-(\nabla\mu,\nabla\mu)=-\|u_t\|_{-1}^2\le 0. \tag{1.5}$$

Eqs. (1.4)-(1.5) indicate that the Allen-Cahn and Cahn-Hilliard equation possess energy-decay property: the total energy is decreasing in time, and the following energy law holds:

$$E(u(t_2))\le E(u(t_1)),\quad \forall t_1<t_2\in(0,T]. \tag{1.6}$$

As two famous phase-field models, the Allen-Cahn equation originated from the work by Allen and Cahn [1] in which a diffusive interfacial model is built to describe the phenomenon of antiphase domain coarsening in a binary alloy. While the Cahn-Hilliard

equation was originally developed by Cahn and Hilliard in [22] to model phase separation and coarsening phenomenon in a non-uniform system. Nowadays, they have been applied to complicated moving interface problems, fluid dynamics and many other problems [4–7, 13–15, 19, 20, 26, 27, 30, 31, 34, 35, 41], due to their advantages in capturing and tracking the interface.

Since the exact solutions of the phase-field equations are not easy to obtain, numerical simulations seem to play a crucial role in the research of the physical problems modeled by the two equations. During the past few years, much work has been paid to the numerical solutions of the Allen-Cahn and Cahn-Hilliard equations. Note that the energy decay property of the phase field equations is considered to be fundamental to their derivation, their behavior, and their discretization, various numerical schemes which satisfy the corresponding discrete energy law have been designed (cf. [9, 23, 24, 32, 34, 37, 39, 40, 48] and the references therein). A commonly used technique to obtain an energy stable discretization includes convex splitting method [3,10,11] and secant-line type method [8,12,19,28]. When applying these schemes for solving the discrete equation, a nonlinear system which is usually of large scale needs to be solved at each time step and some restrictions are imposed on the time step size due to the well posedness of the numerical schemes when second-order time discretization are considered, which are disadvantageous for long-time numerical simulation. In order to overcome these drawbacks, Yang et al. developed a so-called invariant energy quadratization (IEQ) method, which was based on the Lagrange multiplier method introduced in [18], to solve the phase-field models with a large class of free energys [42–47]. In [32, 33], some improvements based on the IEQ method have been made by Shen and his coworkers, and a new method termed as scalar auxiliary variable (SAV) was introduced to deal with gradient flows. Comparing with the IEQ method, the main advantage of the SAV method is that it leads to a linear system with constant coefficients which can be solved efficiently at each time step.

There is another way for developing accurate and efficient numerical methods for phase-field equations. In [5] Chen and Shen introduced a semi-implicit Fourier-spectral method for the phase-field equation, in which the principal elliptic operator is treated implicitly, while the nonlinear terms are still treated explicitly. This treatment leads to a linear system with constant coefficients at each time step, which can be solved efficiently and accurately by the Fourier-spectral method in the case of periodic boundary conditions. Comparing with implicit schemes, semi-implicit schemes suffer from larger truncation errors and a smaller time step needs to be used to preserve the energy decay property. To fully or partially remove these restrictions on time steps, a new range of stabilized semi-implicit scheme was developed. For example, Xu and Tang designed stabilized semi-implicit schemes for epitaxial growth models [38], in which an extra term is added so that a relatively large time step could be utilized for a long-time simulation. A similar stabilized semi-implicit Fourier-spectral method for the Cahn-Hilliard equation was introduced by He et al. [21], in which the energy stability and error estimate for the first order fully discrete scheme are derived based on an assumption that the numerical solution is bounded in maximum norm. In [34] Shen and Yang proposed and analyzed a

series of implicit and stabilized semi-implicit numerical schemes which are unconditionally energy stable or energy stable with reasonable restrictions for the Allen-Cahn and Cahn-Hilliard equations, and optimal error estimates have been derived. All these results have been derived based on a Lipschitz assumption on nonlinearity. This idea was followed up by Feng et al for the analysis of the stabilized Crank-Nicolson scheme for the phase-field equations [17]. While in [29] Li and Qiao proved the unconditional energy stability for the second order in time stabilized semi-implicit Fourier spectral method for the 2D Cahn-Hilliard equation without any prior assumption on the numerical solution or Lipschitz nonlinearity, however, a sufficiently large stabilizing coefficient needs to be used.

In this work, we shall develop two unconditionally energy stable second-order semi-implicit schemes for solving the Allen-Cahn and Cahn-Hilliard equations. One is based on the second order backward differential formula and the other is based on the Crank-Nicolson scheme. In both schemes, the nonlinear term is treated explicitly with a second order extrapolation and a single linear term is added to guarantee the unconditional energy stability so that only a linear system with constant coefficients is derived at each time step. The finite element method has been used for spatial discretization, and priori error estimations are also derived.

The rest of the paper is organized as follows. In Section 2, we consider the stabilized second-order semi-implicit scheme for the Allen-Cahn equation. We show that the second order semi-implicit scheme is unconditionally energy stable, and an error estimate for the fully discrete scheme is also derived. A similar analysis is provided for the Cahn-Hilliard equation in Section 3. We then present some numerical examples in Section 4 for demonstrating the performance of the proposed schemes. Finally, conclusions are drawn in Section 5.

2 Stabilized second order semi-implicit scheme for Allen-Cahn equation

We first introduce some notations which will be used throughout the paper. For a domain $\Omega\subset R^d$, we denote by $\|\cdot\|$ the norm in $L^2=L^2(\Omega)$ which is equipped with L^2 inner product $(\cdot,\cdot)$ and by $\|\cdot\|_r$ that in the Sobolev space $H^r=H^r(\Omega)=W^{r,2}(\Omega)$. For the definition of function spaces L^2 and H^r, we could refer to [2]. The Sobolev space H_0^1 is defined by

$$H_0^1=\{v\in H^1(\Omega):v|_{\partial\Omega}=0\},$$

we also denote the norm in the L^∞ by $\|\cdot\|_\infty$.

For $r\geq 0$, we define

$$H^{-r}(\Omega):=(H^r(\Omega)^*),\quad H_0^{-r}(\Omega):=\{u\in H^{-r}(\Omega)|\langle u,1\rangle_r=0\},$$

where $\langle\cdot,\cdot\rangle_r$ represents the dual product between $H^r(\Omega)$ and $H^{-r}(\Omega)$. Let us denote $L_0^2(\Omega):=H_0^0(\Omega)$. For $w\in L_0^2(\Omega)$, let $w_1=-\Delta^{-1}w\in L_0^2(\Omega)\cap H^1(\Omega)$ satisfy

$$\begin{cases} -\Delta w_1 = w & \text{in } \Omega, \\ \dfrac{\partial w_1}{\partial n} = 0 & \text{on } \partial\Omega, \end{cases} \tag{2.1}$$

and $\|v\|_{-1}=\sqrt{(v,-\Delta^{-1}v)}$.

Based on the above definitions, the weak formulation of the Allen-Cahn equation (1.1) reads: Find $u\in L^2(0,T;H_0^1(\Omega))$ such that

$$(u_t,v)+\epsilon(\nabla u,\nabla v)+(u^3,v)-(u,v)=0,\quad \forall v\in H_0^1(\Omega). \tag{2.2}$$

Next, we subdivide the time interval $[0,T]$ into a partition of N subintervals whose endpoints are denoted by $0=t^0<t^1<\cdots<t^N=T$. For simplicity, we use the uniform mesh for temporal discretization. Let τ be the time step with $t^n=n\tau$, and let u^n be an approximation of the exact solution $u(t^n)$. Based on the second-order backward differential formula, a second-order unconditionally energy stable stabilized semi-implicit scheme is developed for solving the Allen-Cahn equation, given by

$$\begin{aligned}\left(\frac{3u^{n+1}-4u^n+u^{n-1}}{2\tau},q\right) =& -\epsilon(\nabla u^{n+1},\nabla q)-(2f(u^n)-f(u^{n-1}),q)\\ & -A\tau(u^{n+1}-u^n,q),\quad \forall q\in L^2(0,T;H_0^1(\Omega)),\end{aligned} \tag{2.3}$$

where A is a non-negative constant and $f(u)=F'(u)$.

To derive the energy stability of the numerical scheme, following the same arguments in [34], it is reasonable to assume that there exists a positive constant L such that

$$\max_{u\in R}|f'(u)|\le L. \tag{2.4}$$

Remark 2.1. As we all know that the Allen-Cahn equation satisfies the maximum principle, therefore, it has been a common practice (cf. [25,34]) to truncate $F(u)$ to be quadratic for $|u|>M$ (in the case of the Allen-Cahn equation, $M=1$) such that the Lipschitz assumption (2.4) is satisfied. More precisely, we could modify the double-well potential $F(u)=\frac{1}{4}(u^2-1)^2$ by the following truncated function:

$$\tilde{F}(u)=\begin{cases}(u-1)^2, & u>1,\\ \dfrac{1}{4}(u^2-1)^2, & u\in[-1,1],\\ (u+1)^2, & u<-1.\end{cases}$$

Consequently

$$\tilde{f}(u)=\tilde{F}'(u)=\begin{cases}2u-2, & u>1,\\ (u^2-1)u, & u\in[-1,1],\\ 2u+2, & u<-1.\end{cases}$$

And we could take $L=2$ in the calculation of the revised energy $\hat{E}$ for the Allen-Cahn equation.

Theorem 2.1. *Assume* (2.4) *is satisfied, under the condition*

$$A>\frac{9L^2}{16}, \tag{2.5}$$

the following energy stability property holds for the scheme (2.3)*:*

$$\widehat{E}(u^{n+1})\leq\widehat{E}(u^n),\quad \forall n\geq 1, \tag{2.6}$$

where

$$\widehat{E}(u^{n+1})=E(u^{n+1})+\Big(\frac{L}{2}+\frac{1}{4\tau}\Big)\|u^{n+1}-u^n\|^2.$$

Proof. We take $q=u^{n+1}-u^n$ in (2.3) and estimate each term separately as following:

$$\begin{aligned}&\Big(\frac{3u^{n+1}-4u^n+u^{n-1}}{2\tau},u^{n+1}-u^n\Big)=\frac{1}{\tau}(u^{n+1}-u^n+\frac{1}{2}\delta^2u^{n+1},u^{n+1}-u^n)\\ =&\frac{1}{\tau}\|u^{n+1}-u^n\|^2+\frac{1}{4\tau}(\|u^{n+1}-u^n\|^2-\|u^n-u^{n-1}\|^2+\|\delta^2u^{n+1}\|^2),\end{aligned} \tag{2.7}$$

here

$$\delta^2u^{n+1}=u^{n+1}-2u^n+u^{n-1},$$

and we used the following identity:

$$(b^{n+1}-b^n,b^{n+1})=\frac{1}{2}(|b^{n+1}|^2-|b^n|^2+|b^{n+1}-b^n|^2). \tag{2.8}$$

Similarly,

$$\epsilon(\nabla u^{n+1},\nabla(u^{n+1}-u^n))=\frac{\epsilon}{2}(\|\nabla u^{n+1}\|^2-\|\nabla u^n\|^2+\|\nabla(u^{n+1}-u^n)\|^2). \tag{2.9}$$

For the term involving f, using the following Taylor expansion

$$F(u^{n+1})-F(u^n)=f(u^n)(u^{n+1}-u^n)+\frac{f'(\eta^n)}{2}(u^{n+1}-u^n)^2, \tag{2.10}$$

we have

$$\begin{aligned}&(2f(u^n)-f(u^{n-1}),u^{n+1}-u^n)\\ =&\Big(\int_{u^{n-1}}^{u^n}f'(s)ds,u^{n+1}-u^n\Big)+(f(u^n),u^{n+1}-u^n)\\ =&(F(u^{n+1})-F(u^n),1)-\frac{f'(\eta^n)}{2}(u^{n+1}-u^n,u^{n+1}-u^n)+\Big(\int_{u^{n-1}}^{u^n}f'(s)ds,u^{n+1}-u^n\Big).\end{aligned} \tag{2.11}$$

Here η^n lies between u^n and u^{n+1}.

Combining the relations (2.7), (2.9), (2.11), we obtain

$$\begin{aligned}
&E(u^{n+1})-E(u^n)+\Big(A\tau+\frac{1}{\tau}\Big)\|u^{n+1}-u^n\|^2\\
&\quad+\frac{\epsilon}{2}\|\nabla(u^{n+1}-u^n)\|^2+\frac{1}{4\tau}(\|u^{n+1}-u^n\|^2-\|u^n-u^{n-1}\|^2+\|\delta^2u^{n+1})\|^2)\\
=&\frac{f'(\eta^n)}{2}\|u^{n+1}-u^n\|^2-\Big(\int_{u^{n-1}}^{u^n}f'(s)ds,u^{n+1}-u^n\Big)\\
\le&\frac{L}{2}\|u^{n+1}-u^n\|^2+L\|u^n-u^{n-1}\|\|u^{n+1}-u^n\|\\
\le&L\|u^{n+1}-u^n\|^2+\frac{L}{2}\|u^n-u^{n-1}\|^2. \qquad (2.12)
\end{aligned}$$

Here we have used the condition (2.4), the Cauchy-Schwarz inequality and the Young's inequality.

Note that

$$\Big(A\tau+\frac{1}{\tau}\Big)\ge 2\sqrt{A},$$

after dropping some unnecessary terms, we get the desired energy estimate. □

Next, we shall use the finite element method for spatial discretization. Let $\mathcal{T}_h$ be a conforming triangulation of Ω and let S_h be the corresponding finite dimensional space of piecewise linear continuous functions on Ω :

$$S_h=\{v\in H^1(\Omega):v|_\tau\in P_1(\tau),\ \forall\tau\in\mathcal{T}_h\},$$

we also denote

$$S_h^0=S_h\cap H_0^1(\Omega).$$

Consider the fully discretized version of scheme (2.3): Find $u_h^n\in S_h^0$, such that

$$\begin{cases}
\Big(\dfrac{3u_h^{n+1}-4u_h^n+u_h^{n-1}}{2\tau},q_h\Big)=-\epsilon(\nabla u_h^{n+1},\nabla q_h)-(2f(u_h^n)-f(u_h^{n-1}),q_h)\\
\qquad\qquad -A\tau(u_h^{n+1}-u_h^n,q_h),\quad \forall q_h\in L^2(0,T;S_h^0),\\
(u_h^0-u_0,v_h)=0, \qquad\qquad \forall v_h\in S_h^0,
\end{cases} \qquad (2.13)$$

where u_h^0 is an approximation of u_0 in S_h^0.

Note that the scheme (2.13) is a three-level scheme, we apply a second-order unconditionally energy stable scheme [28] to generate u_h^1 from u_h^0:

$$\begin{cases}
\Big(\dfrac{u_h^1-u_h^0}{\tau},v_h\Big)+\epsilon\Big(\nabla\widehat{u_h^1},\nabla v_h\Big)+\Big(f(u_h^1,u_h^0)-\widehat{u_h^1},v_h\Big)=0, \quad \forall v_h\in S_h^0,\\
(u_h^0-u_0,v_h)=0, \qquad\qquad \forall v_h\in S_h^0,
\end{cases} \qquad (2.14)$$

where

$$\widehat{u_h^1}=\frac{u_h^1+u_h^0}{2}, \tag{2.15a}$$

$$f(u_h^1,u_h^0)=\frac{(u_h^1)^3+(u_h^1)^2u_h^0+u_h^1(u_h^0)^2+(u_h^0)^3}{4}. \tag{2.15b}$$

Denote $e^n=u_h^n-u(t^n)$, we shall split the error e^n as following:

$$e^n=u_h^n-I_h(u(t^n))+I_h(u(t^n))-u(t^n)=\hat{e}^n+\tilde{e}^n, \tag{2.16}$$

where I_h is the elliptic projection operator, defined by

$$(\nabla(I_hu-u),\nabla v_h)=0,\quad \forall v_h\in S_h^0. \tag{2.17}$$

Lemma 2.1 ([36]). *With I_hu defined by* (2.17) *and $\tilde{e}=I_hu-u$, assuming $u\in C^2(0,T;H^2(\Omega)\cap H_0^1(\Omega))$, we have*

$$\|\tilde{e}(t)\|+h\|\nabla\tilde{e}(t)\|\le C(u)h^2, \tag{2.18a}$$

$$\|\tilde{e}_t(t)\|+h\|\nabla\tilde{e}_t(t)\|\le C(u)h^2, \tag{2.18b}$$

where $C(u)$ is independent of h.

Now we are ready to give the error estimate for the fully discretized scheme (2.13):

Theorem 2.2. *Let u_h^n and $u(t^n)$ be solution of* (2.13) *and* (1.1) *respectively, and assume that $u\in C^2(0,T;H^2(\Omega)\cap H_0^1(\Omega))$. Then, under the conditions* (2.4) *and* (2.5), *we have*

$$\|u_h^n-u(t^n)\|\le C\|u_h^0-u_0\|+C(h^2+\tau^2), \tag{2.19}$$

where C is a positive constant that depend on ϵ, L, A, T, u.

Proof. From (2.16) and note that $\tilde{e}^n$ is bounded according to Lemma 2.1. It remains to estimate $\hat{e}^n$. Denote

$$\bar{\partial}u_h^{n+1}=\frac{3u_h^{n+1}-4u_h^n+u_h^{n-1}}{2\tau},\quad \hat{f}_h^{n+1}=2f(u_h^n)-f(u_h^{n-1}),\quad \hat{f}^{n+1}=2f(u(t^n))-f(u(t^{n-1})).$$

We have

$$\begin{aligned}
&(\bar{\partial}\hat{e}^{n+1},\chi)+\varepsilon(\nabla\hat{e}^{n+1},\nabla\chi)\\
=&(\bar{\partial}u_h^{n+1},\chi)+\varepsilon(\nabla u_h^{n+1},\nabla\chi)-(\bar{\partial}I_hu(t^{n+1}),\chi)-\varepsilon(\nabla I_hu(t^{n+1}),\nabla\chi)\\
=&-(\hat{f}_h^{n+1},\chi)-A\tau(u_h^{n+1}-u_h^n,\chi)-(u_t(t^{n+1}),\chi)-(\bar{\partial}I_hu(t^{n+1})-u_t(t^{n+1}),\chi)\\
&-\varepsilon(\nabla I_hu(t^{n+1}),\nabla\chi)\\
=&(f(u(t^{n+1}))-\hat{f}_h^{n+1},\chi)-(\bar{\partial}I_hu(t^{n+1})-u_t(t^{n+1}),\chi)-A\tau(u_h^{n+1}-u_h^n,\chi),\quad \forall\chi\in S_h^0.
\end{aligned} \tag{2.20}$$

Applying Lemma 2.1, Taylor expansion and condition (2.4) we have:

$$\begin{aligned}
&\|f(u(t^{n+1}))-\hat{f}_h^{n+1}\|\\
=&\|f(u(t^{n+1}))-\hat{f}^{n+1}+\hat{f}^{n+1}-\hat{f}_h^{n+1}\|\\
\leq&\|f(u(t^{n+1}))-f(u(t^n))+f(u(t^{n-1}))-f(u(t^n))\|\\
&+\|2(f(u(t^n))-f(u_h^n))\|+\|(f(u(t^{n-1})-f(u_h^{n-1}))\|\\
\leq&\|f'(u)(u(t^{n+1})-2u(t^n)+u(t^{n-1}))\|+\|6\xi_1(u(t^{n+1})-u(t^n))^2\|\\
&+\|6\xi_2(u(t^n)-u(t^{n-1}))^2\|+2L\|\hat{e}^n+\tilde{e}^n\|+L\|\hat{e}^{n-1}+\tilde{e}^{n-1}\|\\
\leq&C(u,L)(\tau^2+h^2)+C(\|\hat{e}^n\|+\|\hat{e}^{n+1}\|+\|\hat{e}^{n-1}\|),
\end{aligned}\tag{2.21}$$

where ξ_1 lies between $u(t^{n+1})$ and $u(t^n)$, ξ_2 lies between $u(t^n)$ and $u(t^{n-1})$

$$\begin{aligned}
\|\bar{\partial}I_h u(t^{n+1})-u_t(t^{n+1})\|&=\|\bar{\partial}I_h u(t^{n+1})-\bar{\partial}u(t^{n+1})+\bar{\partial}u(t^{n+1})-u_t(t^{n+1})\|\\
&\leq\|\bar{\partial}\tilde{e}^{n+1}\|+\|\bar{\partial}u(t^{n+1})-u_t(t^{n+1})\|\\
&\leq C(u)(h^2+\tau^2),
\end{aligned}\tag{2.22a}$$

$$\begin{aligned}
A\tau\|u_h^{n+1}-u_h^n\|&=A\tau\|u_h^{n+1}-u(t^{n+1})+u(t^{n+1})-u(t^n)+u(t^n)-u_h^n\|\\
&\leq A\tau(\|\hat{e}^n\|+\|\hat{e}^{n+1}\|)+C(u)(\tau^2+h^2).
\end{aligned}\tag{2.22b}$$

Then we turn our attention to (2.20). Setting $\chi=\hat{e}^{n+1}$, we obtain

$$\begin{aligned}
&(\bar{\partial}\hat{e}^{n+1},\hat{e}^{n+1})+\varepsilon\|\nabla\hat{e}^{n+1}\|^2\\
\leq&(\|f(u(t^{n+1}))-\hat{f}_h^{n+1}\|+A\tau\|u_h^{n+1}-u_h^n\|+\|\bar{\partial}I_h u(t^{n+1})-u_t(t^{n+1})\|)\|\nabla\hat{e}^{n+1}\|,
\end{aligned}$$

where we have used Friedrichs' inequality $\|\hat{e}^n\|\leq C\|\nabla\hat{e}^n\|$. And hence

$$\begin{aligned}
&(\bar{\partial}\hat{e}^{n+1},\hat{e}^{n+1})\\
\leq&C(\varepsilon^{-1})(\|f(u(t^{n+1}))-\hat{f}_h^{n+1}\|^2+A^2\tau^2\|u_h^{n+1}-u_h^n\|^2+\|\bar{\partial}I_h u(t^{n+1})-u_t(t^{n+1}))\|^2.
\end{aligned}\tag{2.23}$$

Substituting (2.21)-(2.22b) into (2.23), we have

$$(\bar{\partial}\hat{e}^{n+1},\hat{e}^{n+1})\leq C(\varepsilon^{-1})(\|\hat{e}^{n-1}\|^2+\|\hat{e}^n\|^2+\|\hat{e}^{n+1}\|^2)+C(u,L)(\tau^2+h^2)^2.\tag{2.24}$$

Note that

$$\begin{aligned}
(\bar{\partial}\hat{e}^{n+1},\hat{e}^{n+1})=&\frac{1}{4\tau}(|\hat{e}^{n+1}|^2+|2\hat{e}^{n+1}-\hat{e}^n|^2)\\
&-\frac{1}{4\tau}(|\hat{e}^n|^2+|2\hat{e}^n-\hat{e}^{n-1}|^2-|\hat{e}^{n+1}-2\hat{e}^n+\hat{e}^{n-1}|^2)\\
\geq&\frac{1}{4\tau}(|\hat{e}^{n+1}|^2-|\hat{e}^n|^2-|2\hat{e}^n-\hat{e}^{n-1}|^2),
\end{aligned}\tag{2.25}$$

where we have used the following identity:

$$\begin{aligned}&2a^{k+1}(3a^{k+1}-4a^k+2a^{k-1})\\=&|a^{k+1}|^2+|2a^{k+1}-a^k|^2-|a^k|^2-|2a^k-a^{k-1}|^2-|a^{k+1}-2a^k+a^{k-1}|^2.\end{aligned}$$

Substitute (2.25) into (2.24), we have

$$\frac{\|\hat{e}^{n+1}\|^2-\|\hat{e}^n\|^2}{\tau}\leq C(T,\varepsilon^{-1})(\|\hat{e}^{n-1}\|^2+\|\hat{e}^n\|^2+\|\hat{e}^{n+1}\|^2)+C(u,L)(\tau^2+h^2)^2. \tag{2.26}$$

Multiplying (2.26) with τ and summing up the inequality for $1\leq n\leq N-1$, we obtain

$$(1-C\tau)\|\hat{e}^{n+1}\|^2\leq C(T,\varepsilon^{-1})\sum_{n=1}^{N-1}(\|\hat{e}^n\|^2+\|\hat{e}^{n-1}\|^2)+C(u,L)(\tau^2+h^2)^2. \tag{2.27}$$

The desired estimate (2.19) then followed by the discrete Gronwall's inequality and the triangular inequality $\|e^n\|^2\leq\|\tilde{e}^n\|^2+\|\hat{e}^n\|^2$. □

3 Stabilized second order semi-implicit scheme for Cahn-Hilliard equation

In this section, we consider the Cahn-Hilliard equation (1.2), and its mixed variational formula reads: Find $u,\mu\in L^2(0,T;H^1(\Omega))$ such that

$$\begin{cases}\left(\dfrac{\partial u}{\partial t},q\right)-(\nabla\mu,\nabla q)=0 & \text{for all}\quad q\in L^2(0,T;H^1(\Omega)),\\ \epsilon(\nabla u,\nabla v)+(F'(u),v)=-(\mu,v) & \text{for all}\quad v\in L^2(0,T;H^1(\Omega)).\end{cases} \tag{3.1}$$

Based on the Crank-Nicolson scheme, a second order unconditionally energy stable stabilized semi-implicit scheme is developed for solving the problem (1.2), given by

$$\begin{cases}\left(\frac{u^{n+1}-u^n}{\tau},q\right)-\left(\nabla\mu^{n+\frac{1}{2}},\nabla q\right)=0, & \forall q\in L^2(0,T;H^1(\Omega)),\\ \epsilon\left(\nabla\left(\dfrac{u^{n+1}+u^n}{2}\right),\nabla v\right)+\left(\dfrac{3}{2}f(u^n)-\dfrac{1}{2}f(u^{n-1}),v\right) & \\ \quad+A\tau(\nabla(u^{n+1}-u^n),\nabla v)=-(\mu^{n+\frac{1}{2}},v), & \forall v\in L^2(0,T;H^1(\Omega)),\end{cases} \tag{3.2}$$

where A is a non-negative constant,

$$\mu^n=\epsilon\Delta u^n-F'(u^n),\quad \mu^{n+\frac{1}{2}}=\frac{1}{2}(\mu^n+\mu^{n+1}).$$

Note that the stabilized Crank-Nicolson scheme (3.2) is also a three-level scheme, the unconditionally energy stable scheme (2.14) is generalized for solving Cahn-Hilliard

equation (1.2) (see also [8, 12]) to generate u^1, given by

$$\begin{cases} \left(\frac{u^1-u^0}{\tau},q\right)-\left(\nabla\mu^{\frac{1}{2}},\nabla q\right)=0, & \forall q\in L^2(0,T;H^1(\Omega)), \\ \varepsilon\left(\nabla\left(\frac{u^1+u^0}{2}\right),\nabla v\right)+(f(u^1,u^0),v)=-(\mu^{\frac{1}{2}},v), & \forall v\in L^2(0,T;H^1(\Omega)), \end{cases} \tag{3.3}$$

where $f(u^1,u^0)$ is defined as following:

$$f(u^1,u^0)=\frac{(u^1)^3+(u^1)^2u^0+u^1(u^0)^2+(u^0)^3}{4}-\frac{u^1+u^0}{2}.$$

Suppose the initial value u^0 satisfies the following condition:

$$\frac{1}{|\Omega|}\int_\Omega u^0dx=M_0 \tag{3.4}$$

under the homogeneous Neumann boundary condition of μ, it is easy to check that

$$\frac{1}{|\Omega|}\int_\Omega u^1dx=M_0. \tag{3.5}$$

Theorem 3.1. *Assume* (3.4) *and* (2.4) *is satisfied, then under the condition*

$$A>\frac{L^2}{2}, \tag{3.6}$$

the following energy stability property holds for the scheme (3.2)*:*

$$\tilde{E}(u^{n+1})+\frac{\tau}{2}\|\nabla\mu^{n+1}\|^2\le\tilde{E}(u^n),\quad \forall n\ge1, \tag{3.7}$$

where

$$\tilde{E}(u^{n+1})=E(u^{n+1})+\frac{L}{4}\|u^{n+1}-u^n\|^2.$$

Proof. It is easy to verify that under the condition (3.4), we have

$$\frac{1}{|\Omega|}\int_\Omega u^{n+1}dx=M_0,\quad n=1,2,\cdots,N-1. \tag{3.8}$$

Hence, $u^{n+1}-u^n\in L_0^2(\Omega)$, $n=0,1,\cdots,N$.

On taking

$$q=-\frac{\tau}{2}\mu^{n+\frac{1}{2}}\quad\text{and}\quad v=u^{n+1}-u^n$$

in (3.2), and combining the results, we get

$$\frac{1}{2}(u^{n+1}-u^n,\mu^{n+\frac{1}{2}})+\frac{\tau}{2}\|\nabla\mu^{n+\frac{1}{2}}\|^2+\frac{\epsilon}{2}(\|\nabla u^{n+1}\|^2-\|\nabla u^n\|^2)$$
$$+\left(\frac{3}{2}f(u^n)-\frac{1}{2}f(u^{n-1}),u^{n+1}-u^n\right)=-A\tau\|\nabla(u^{n+1}-u^n)\|^2. \tag{3.9}$$

Taking

$$q=-\frac{1}{2}\Delta^{-1}(u^{n+1}-u^n),$$

we obtain

$$\frac{1}{2\tau}\|u^{n+1}-u^n\|_{-1}^2-\frac{1}{2}(\mu^{n+\frac{1}{2}},u^{n+1}-u^n)=0. \tag{3.10}$$

To handle the nonlinear term, from the Taylor expansion (2.10), we have

$$\left(\frac{3}{2}f(u^n)-\frac{1}{2}f(u^{n-1}),u^{n+1}-u^n\right)$$
$$=(F(u^{n+1})-F(u^n),1)-\frac{f'(\eta^n)}{2}(u^{n+1}-u^n,u^{n+1}-u^n)$$
$$+\frac{1}{2}\left(\int_{u^{n-1}}^{u^n}f'(s)ds,u^{n+1}-u^n\right). \tag{3.11}$$

Combining the relation (3.9)-(3.11) and condition (2.4), we obtain

$$\frac{\tau}{2}\|\nabla\mu^{n+\frac{1}{2}}\|^2+E(u^{n+1})-E(u^n)$$
$$\leq-A\tau\|\nabla(u^{n+1}-u^n)\|^2-\frac{1}{2\tau}\|u^{n+1}-u^n\|_{-1}^2$$
$$+\frac{3L}{4}\|u^{n+1}-u^n\|^2+\frac{L}{4}\|u^n-u^{n-1}\|^2. \tag{3.12}$$

Note that

$$-A\tau\|\nabla(u^{n+1}-u^n)\|^2-\frac{1}{2\tau}\|u^{n+1}-u^n\|_{-1}^2\leq-\sqrt{2A}\|(u^{n+1}-u^n)\|^2. \tag{3.13}$$

Substituting the inequality (3.13) into (3.12), and we get the desired energy estimate. □

Let us define error function $\bar{e}^n=u(t^n)-u^n$, to derive the error estimate of the above scheme, we shall make some assumptions for some initial values:

We suppose u^0=$u(t^0)$ and assume that when the unconditionally energy stable scheme (3.3) is used to solve (1.2) at first step, there exists a positive constant C_1 independent of τ such that

$$\epsilon\tau\|\nabla\bar{e}^1\|^2\leq C_1\tau^4, \tag{3.14}$$

and the following inequality will be used frequently:

$$(u,v)\leq\|u\|_{-1}\|\nabla v\|,\quad u\in L_0^2,\quad v\in H^1. \tag{3.15}$$

Theorem 3.2. *Let $u(t^n)$ and u^n be solution of* (1.2) *and* (3.3) *respectively, and suppose A satisfy the following constraint*

$$A \geq \max\left\{1, \frac{L^2}{2}\right\},$$

then for $u_{ttt} \in L^2(0,T;H^{-1}(\Omega))$, $u_{tt} \in L^2(0,T;H^3(\Omega))$, $u_t \in L^2(0,T;H^3(\Omega))$, under the conditions (2.4) *and* (3.14)*, we have*

$$\begin{aligned}&\sum_{n=1}^{N-1}\left\{\|\bar{e}^{n+1}-\bar{e}^n\|_{-1}^2+(A-1)\tau^2\|\nabla(\bar{e}^{n+1}-\bar{e}^n)\|^2\right\}\\&\quad+\max_{1\leq n\leq N-1}\left\{\frac{\epsilon\tau}{2}\|\nabla\bar{e}^{n+1}\|^2\right\}\leq C_1e^{C_2}\tau^4,\end{aligned}\tag{3.16}$$

where C_1, C_2 are two positive constants depending on ϵ, A, L, T.

Proof. Substracting (3.3) from (1.2) at $t^{n+\frac{1}{2}}$ gives

$$\left(\frac{\bar{e}^{n+1}-\bar{e}^n}{\tau},q\right)-\left(\nabla(\mu(t^{n+\frac{1}{2}})-\mu^{n+\frac{1}{2}}),\nabla q\right)=(T_1^{n+\frac{1}{2}},q),\tag{3.17a}$$

$$\begin{aligned}&\varepsilon\left(\nabla(\frac{\bar{e}^{n+1}+\bar{e}^n}{2}),\nabla v\right)+\left(f(u(t^{n+\frac{1}{2}}))-\frac{3}{2}f(u^n)+\frac{1}{2}f(u^{n-1}),v\right)\\&=\varepsilon(T_2^{n+\frac{1}{2}},v)-A\tau(\nabla(\bar{e}^{n+1}-\bar{e}^n),\nabla v)+A(\nabla T_3^{n+1},\nabla v)\\&\quad-\left(\mu(t^{n+\frac{1}{2}})-\mu^{n+\frac{1}{2}},q\right),\end{aligned}\tag{3.17b}$$

where

$$\begin{aligned}&T_1^{n+\frac{1}{2}}:=\frac{u(t^{n+1})-u(t^n)}{\tau}-u_t(t^{n+\frac{1}{2}}),\\&T_2^{n+\frac{1}{2}}:=\Delta u(t^{n+\frac{1}{2}})-\Delta\left(\frac{u(t^{n+1})+u(t^n)}{2}\right),\\&T_3^{n+1}:=\tau(u(t^{n+1})-u(t^n)).\end{aligned}$$

By using the Taylor expansion with integral residual, it is easy to show that

$$\|T_1^{n+\frac{1}{2}}\|_{-1}^2\leq c_1\tau^3\int_{t^n}^{t^{n+1}}\|u_{ttt}(t)\|_{-1}^2dt,\tag{3.18a}$$

$$\|\nabla T_2^{n+\frac{1}{2}}\|^2\leq c_2\tau^3\int_{t^n}^{t^{n+1}}\|\nabla\Delta u_{tt}(t)\|^2dt,\tag{3.18b}$$

$$\|\nabla\Delta T_3^{n+1}\|^2\leq c_3\tau^3\int_{t^n}^{t^{n+1}}\|\nabla\Delta u_t(t)\|^2dt,\tag{3.18c}$$

where c_1, c_2 and c_3 are three positive constants.

Taking $q=-\tau\Delta^{-1}(\bar{e}^{n+1}-\bar{e}^n)$ in (3.17a) and $v=\tau(\bar{e}^{n+1}-\bar{e}^n)$ in (3.17b), and then summing up the resulting identities, we obtain

$$\begin{aligned}&\|\bar{e}^{n+1}-\bar{e}^n\|_{-1}^2+\frac{\epsilon}{2}\tau(\|\nabla\bar{e}^{n+1}\|^2-\|\nabla\bar{e}^n\|^2)+A\tau^2\|\nabla(\bar{e}^{n+1}-\bar{e}^n)^2\|\\ =&\tau(T_1^{n+\frac{1}{2}},-\Delta^{-1}(\bar{e}^{n+1}-\bar{e}^n))+\tau\epsilon(T_2^{n+\frac{1}{2}},\bar{e}^{n+1}-\bar{e}^n)+A\tau(\nabla T_3^{n+1},\nabla(\bar{e}^{n+1}-\bar{e}^n))\\ &-\tau(f(u(t^{n+\frac{1}{2}}))-\frac{3}{2}f(u^n)+\frac{1}{2}f(u^{n-1}),\bar{e}^{n+1}-\bar{e}^n)=\sum_{j=1}^4 R_j.\end{aligned}\tag{3.19}$$

Next we will estimate the right terms R_j, $j=1,\cdots,4$, and we will denote by C a generic constant whose value may vary from line to line.

Using Young's inequality, inequality (3.15), and estimates (3.18)-(3.18c), we obtain:

$$\begin{aligned}R_1\le&\tau\|T_1^{n+\frac{1}{2}}\|_{-1}^2+\frac{\tau}{4}\|\bar{e}^{n+1}-\bar{e}^n\|_{-1}^2\\ \le&C\tau^4\int_{t^n}^{t^{n+1}}\|u_{ttt}(s)\|_{-1}^2ds+\frac{\tau}{4}\|\bar{e}^{n+1}-\bar{e}^n\|_{-1}^2,\end{aligned}\tag{3.20a}$$

$$\begin{aligned}R_2\le&\epsilon^2\tau\|\nabla T_2^{n+\frac{1}{2}}\|^2+\frac{\tau}{4}\|\bar{e}^{n+1}-\bar{e}^n\|_{-1}^2\\ \le&C\epsilon^2\tau^4\int_{t^n}^{t^{n+1}}\|\nabla\Delta u_{tt}(s)\|^2ds+\frac{\tau}{4}\|\bar{e}^{n+1}-\bar{e}^n\|_{-1}^2,\end{aligned}\tag{3.20b}$$

$$\begin{aligned}R_3\le&C(A,T)\tau\|\nabla\Delta T_3^{n+1}\|^2+\frac{\tau}{4}\|\bar{e}^{n+1}-\bar{e}^n\|_{-1}^2\\ \le&C(A,T)\tau^4\int_{t^n}^{t^{n+1}}\|\nabla\Delta u_t(s)\|^2ds+\frac{\tau}{4}\|\bar{e}^{n+1}-\bar{e}^n\|_{-1}^2,\end{aligned}\tag{3.20c}$$

$$\begin{aligned}R_4=&\tau(I_1+I_2+I_3,\bar{e}^{n+1}-\bar{e}^n)\\ \le&\tau\|\nabla I_1\|^2+\frac{\tau}{4}\|\bar{e}^{n+1}-\bar{e}^n\|_{-1}^2+C(T)\tau\|I_2\|_{-1}^2+\frac{\tau^2}{2}\|\nabla(\bar{e}^{n+1}-\bar{e}^n)\|^2\\ &+C(T)\tau\|I_3\|_{-1}^2+\frac{\tau^2}{2}\|\nabla(\bar{e}^{n+1}-\bar{e}^n)\|^2\\ \le&C\tau^4\int_{t^{n-1}}^{t^{n+1}}\|\nabla u_{tt}(s)\|^2ds+\frac{\tau}{4}\|\bar{e}^{n+1}-\bar{e}^n\|_{-1}^2+C(L,T)\tau\|\bar{e}^n\|_{-1}^2\\ &+C(L,T)\tau\|\bar{e}^{n-1}\|_{-1}^2+\tau^2\|\nabla(\bar{e}^{n+1}-\bar{e}^n)\|^2,\end{aligned}\tag{3.20d}$$

where

$$I_1:=f(u(t^{n+\frac{1}{2}}))-\bar{f}(u(t^{n+\frac{1}{2}}))+\bar{f}(u(t^{n+\frac{1}{2}}))-\frac{3}{2}f(u(t^n))+\frac{1}{2}f(u(t^{n-1})),\tag{3.21a}$$

$$I_2:=\frac{3}{2}f(u(t^n))-\frac{3}{2}f(u^n)\quad I_3:=\frac{1}{2}f(u^{n-1})-\frac{1}{2}f(u(t^{n-1})),\tag{3.21b}$$

$$\bar{f}(u(t^{n+\frac{1}{2}})):=\frac{1}{2}(f(u(t^n))+f(u(t^{n+1}))).\tag{3.21c}$$

Combining the above estimates into (3.19) yields

$$\begin{aligned}
&\|\bar{e}^{n+1}-\bar{e}^{n}\|_{-1}^2+\frac{\epsilon\tau}{2}(\|\nabla\bar{e}^{n+1}\|^2-\|\nabla\bar{e}^{n}\|^2)+(A-1)\tau^2\|\nabla(\bar{e}^{n+1}-\bar{e}^{n})\|\\
\leq& C\tau^4\int_{t^n}^{t^{n+1}}\|u_{ttt}(s)\|_{-1}^2ds+C\epsilon^2\tau^4\int_{t^n}^{t^{n+1}}\|\nabla\Delta u_{tt}(s)\|^2ds+C(A,T)\tau^4\int_{t^n}^{t^{n+1}}\|\nabla\Delta u_t(s)\|^2ds\\
&+C\tau^4\int_{t^{n-1}}^{t^{n+1}}\|\nabla u_{tt}(s)\|^2)ds+C\tau(|\bar{e}^{n+1}\|_{-1}^2+\|\bar{e}^{n}\|_{-1}^2+\|\bar{e}^{n-1}\|_{-1}^2). \qquad (3.22)
\end{aligned}$$

On summing up the above inequality for $1\leq n\leq N-1$, we arrive at

$$\begin{aligned}
&\sum_{n=1}^{N-1}(\|\bar{e}^{n+1}-\bar{e}^{n}\|_{-1}^2+(A-1)\tau^2\|\nabla(\bar{e}^{n+1}-\bar{e}^{n})\|^2)+\frac{\epsilon\tau}{2}(\|\nabla\bar{e}^{N}\|^2-\|\nabla\bar{e}^{1}\|^2)\\
\leq& C\tau^4\|u_{ttt}\|_{L^2(0,T;H^{-1})}^2+\epsilon^2\tau^4\|u_{tt}\|_{L^2(0,T;H^3)}^2+C(A,T)\tau^4\|u_t\|_{L^2(0,T;H^3)}^2\\
&+C\tau^4\|u_{tt}\|_{L^2(0,T;H^1)}^2+C\tau\sum_{n=1}^{N-1}(\|\bar{e}^{n+1}\|_{-1}^2+\|\bar{e}^{n}\|^2+\|\bar{e}^{n-1}\|^2). \qquad (3.23)
\end{aligned}$$

The estimate (3.16) then follows by assumption (3.14) and the discrete Gronwall inequality. □

4 Numerical results

In this section, some numerical examples are presented to illustrate the accuracy and the energy stability of the proposed schemes. In our experiments in two dimensions, uniform triangulations will be adopted. Our uniform mesh is generated as follows: first we partition the computational domain Ω into $N\times N$ rectangles, and then partition each rectangle into two right-angled triangles.

4.1 Allen-Cahn equation

Example 4.1. In this example, we test the numerical accuracy for the energy stable scheme (2.13). We consider the following homogeneous Allen-Cahn equation whose solution has been constructed

$$\begin{cases}
\dfrac{\partial u}{\partial t}-\epsilon\Delta u+F'(u)=f, & (x,t)\in\Omega\times(0,T],\\
u(x,t)=0, & (x,t)\in\partial\Omega\times(0,T],\\
u(x,0)=u_0(x), & x\in\Omega,
\end{cases} \qquad (4.1)$$

with $\epsilon=0.01$ and $\Omega=(0,1)^2$. The exact solution is

$$u=t^2\sin(\pi x_1)\sin(\pi x_2),$$

Table 1: Example 4.1. Errors and convergence rate of the spatial discretization accuracy test for scheme (2.13), $A=1$, $T=0.1,0.5,1$.

h	$T=0.1$				$T=0.5$				$T=1$			
	$\|u-u_h\|_{L^2}$	order	$\|u-u_h\|_{H^1}$	order	$\|u-u_h\|_{L^2}$	order	$\|u-u_h\|_{H^1}$	order	$\|u-u_h\|_{L^2}$	order	$\|u-u_h\|_{H^1}$	order
1/40	1.12e-04	\	1.00e-03	\	7.32e-05	\	2.18e-02	\	2.44e-04	\	8.73e-02	\
1/80	2.77e-05	2.01	4.56e-04	1.13	1.80e-05	2.02	1.09e-02	1.00	6.17e-05	1.98	4.36e-02	1.00
1/160	6.90e-06	2.00	2.21e-04	1.04	4.47e-06	2.01	5.50e-03	0.99	1.55e-05	1.99	2.18e-02	1.00
1/320	1.72e-06	2.00	1.09e-04	1.01	1.11e-06	2.01	2.70e-03	1.03	3.90e-06	1.99	1.09e-02	1.00
1/640	4.30e-07	2.00	5.45e-05	1.00	2.78e-07	2.00	1.35e-03	1.00	9.76e-07	2.00	5.50e-03	0.99

Table 2: Example 4.1. Errors and convergence rate of the temporal discretization accuracy test for scheme (2.13), $A=1$, $T=0.1,0.5,1$.

τ	$T=0.1$		$T=0.5$		$T=1$	
	$\|u-u_h\|_{L^2}$	order	$\|u-u_h\|_{L^2}$	order	$\|u-u_h\|_{L^2}$	order
1/40	7.32e-05	\	2.78e-04	\	7.04e-04	\
1/80	1.80e-05	2.03	7.00e-05	1.99	1.86e-04	1.91
1/160	4.47e-06	2.01	1.64e-05	2.10	4.80e-05	1.96
1/320	1.11e-06	2.01	4.06e-06	2.04	1.21e-05	1.99
1/640	2.78e-07	2.00	1.00e-06	2.02	3.02e-06	2.00

the initial condition u_0 and the source f can be chosen to satisfy (4.1).

We first test the accuracy on the spatial discretization by taking the time step size $\tau=\frac{h}{2}$. The errors at time $T=0.1,0.5,1$ with different spatial mesh size h are shown in Table 1, we see clearly that the order of convergence of the errors $\|u-u_h\|_{L^2(\Omega)}$ and $|u-u_h|_{H^1(\Omega)}$ are 2 and 1, respectively. Next, we test the accuracy of the temporal discretization with a spatial mesh size $h=1.0e-03$. The L^2- norm errors at $T=0.1,0.5,1$ and the corresponding convergence rates are shown in Table 2, numerical results show that the convergence rate for time discretization is 2. These results are in consistence with the theory established in Section 2.

Example 4.2. In this example, we consider the Allen-Cahn equation (1.1). The initial condition is chosen such that

$$u_0(x_1,x_2)=0.05\sin x_1\cdot\sin x_2.$$

The parameter is chosen as $\epsilon=0.01$, the solution domain $\Omega=(0,2\pi)\times(0,2\pi)$.

We numerically investigate the performance of the energy stable scheme (2.13) on the above problem with $h=\frac{1}{64}$, $\tau=\frac{1}{2}$, and compute $u(x,t)$ for $0<t\leq 900$. In Fig. 1, the time evolution of the discrete original energy $E(u^n)$ and discrete revised energy $\hat{E}(u^n)$ with different time steps are plotted. It shows that both the original energy and the revised energy decrease with respect to time. The time history of the supremum norms of the numerical solutions is also presented in Fig. 1, in which we can observe that the supremum norms of the numerical solutions are always bounded by 1. We also present the numerical solutions at times $t=1,10,60,550,800,900$ in Fig. 2. We notice that the figure

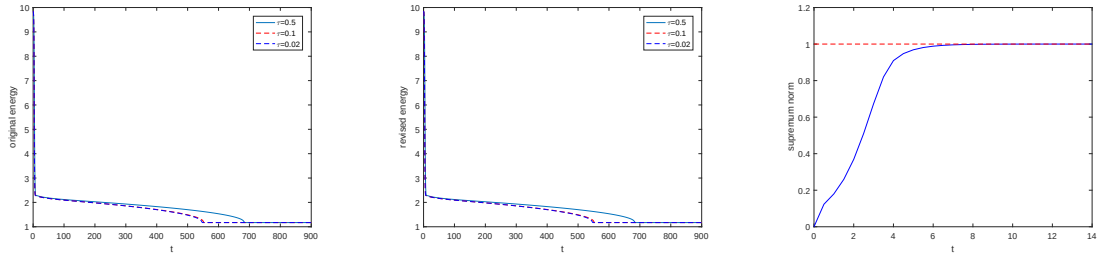

(a) (b) (c)

Figure 1: Example 4.2. $N=64$, $\tau=\frac{1}{2}$ and $A=1$, (a): time evolution of the discrete original energy; (b): time evolution of the discrete revised energy; (c): time history of supremum norm.

changed greatly in a very short period of time, and then the figure changed slowly in a relatively long period of time, and finally the figure tends to be stable, which coincides with the trend of the energy curve.

Example 4.3. In this example, we consider the three-dimensional Allen-Cahn equation:

$$\begin{cases} \dfrac{\partial u}{\partial t}-\Delta u+\dfrac{1}{\varepsilon^2}F'(u)=0, & (x,t)\in\Omega\times(0,T], \\ u(x,0)=u_0(x), & x\in\Omega, \\ \dfrac{\partial u}{\partial n}=0, & (x,t)\in\partial\Omega\times(0,T], \end{cases} \tag{4.2}$$

where $\Omega=[-1,1]^3$, $\epsilon=0.05$ and

$$u_0(x_1,x_2,x_3)=\varepsilon\cos(1.5\pi x_1)\cos(1.5\pi x_2)(\sin(\pi x_3)+\sin(2\pi x_3)).$$

To obtain the numerical solution, the computational domain Ω was meshed with tetrahedral elements with mesh size $h=0.1$, and our energy stable scheme (2.13) was applied to solve the above problem with $\tau=1.0e-04$. The snapshots of numerical solutions at several different moments are presented in Fig. 3 and the evolution of discrete energy and supremum norms are shown in Fig. 4. Same as the previous experiment in two dimensions, the supremum norms of numerical solutions are controlled and the discrete energy is always dissipative.

4.2 Cahn-Hilliard equation

Example 4.4. In this example, we consider the energy stable scheme (3.14) for the following Cahn-Hilliard equation:

$$\begin{cases} \dfrac{\partial u}{\partial t}-\Delta(-\epsilon\Delta u+F'(u))=f, & (x,t)\in\Omega\times(0,T], \\ u(x,0)=u_0(x), & x\in\Omega, \\ \partial_n u=\partial_n\Delta u=0, & (x,t)\in\partial\Omega\times(0,T], \end{cases} \tag{4.3}$$

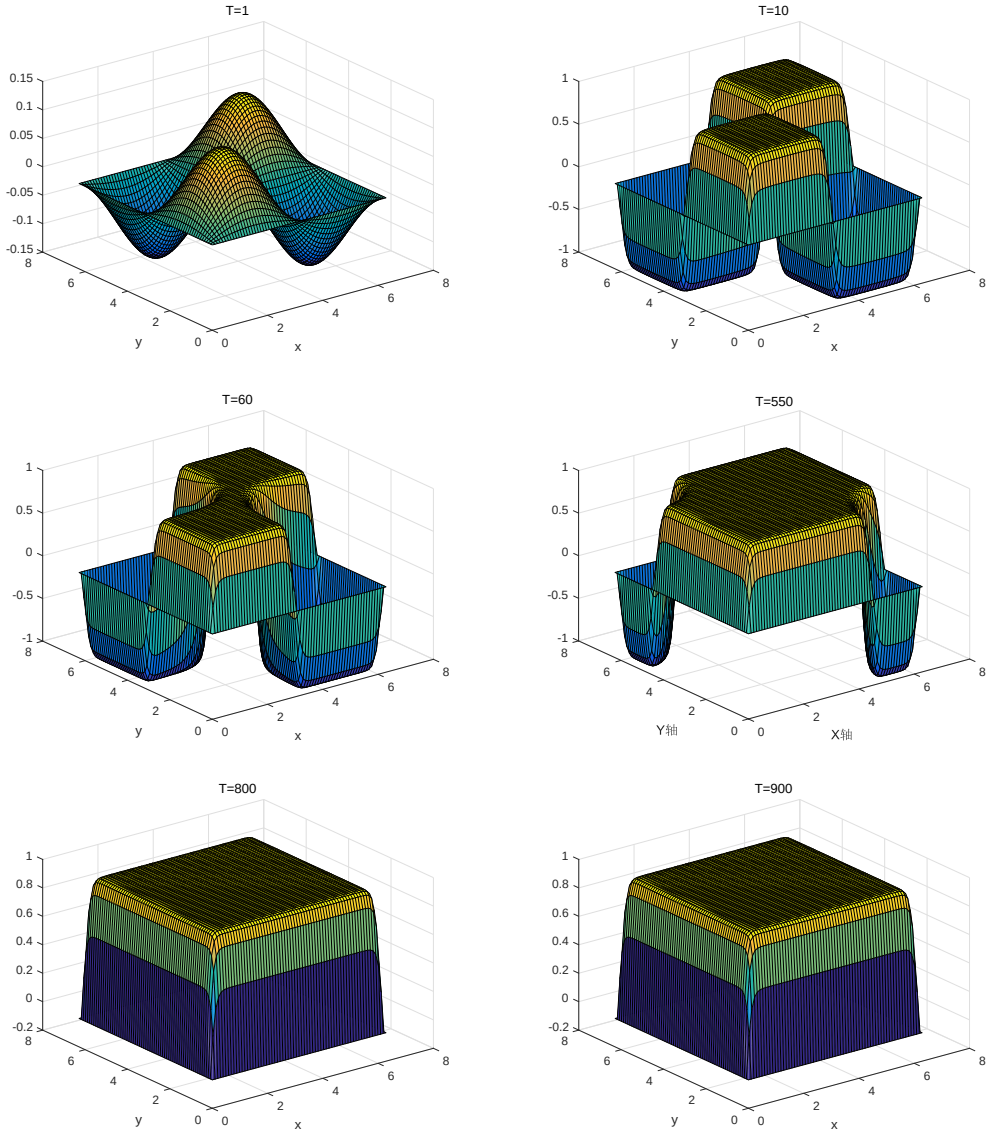

Figure 2: Example 4.2, $N=64$, $\tau=\frac{1}{2}$ and $A=1$, the numerical solutions at $t=1,10,60,550,800,900$.

where $\epsilon=0.1$, $\Omega=[0,1]$. The initial solution u_0 and function f are chosen such that the exact solution is $u(x,t)=e^{-t}\cos(\pi x)$.

We begin to test the accuracy on the spatial discretization with the time step size $\tau=1.0e-06$. The numerical errors at $T=0.1$ with different spatial mesh size are reported in Table 3, which shows that the L^2-norm errors convergent with order 2 while the H^1-seminorm errors convergent with order 1. Then we test the convergence rate with respect

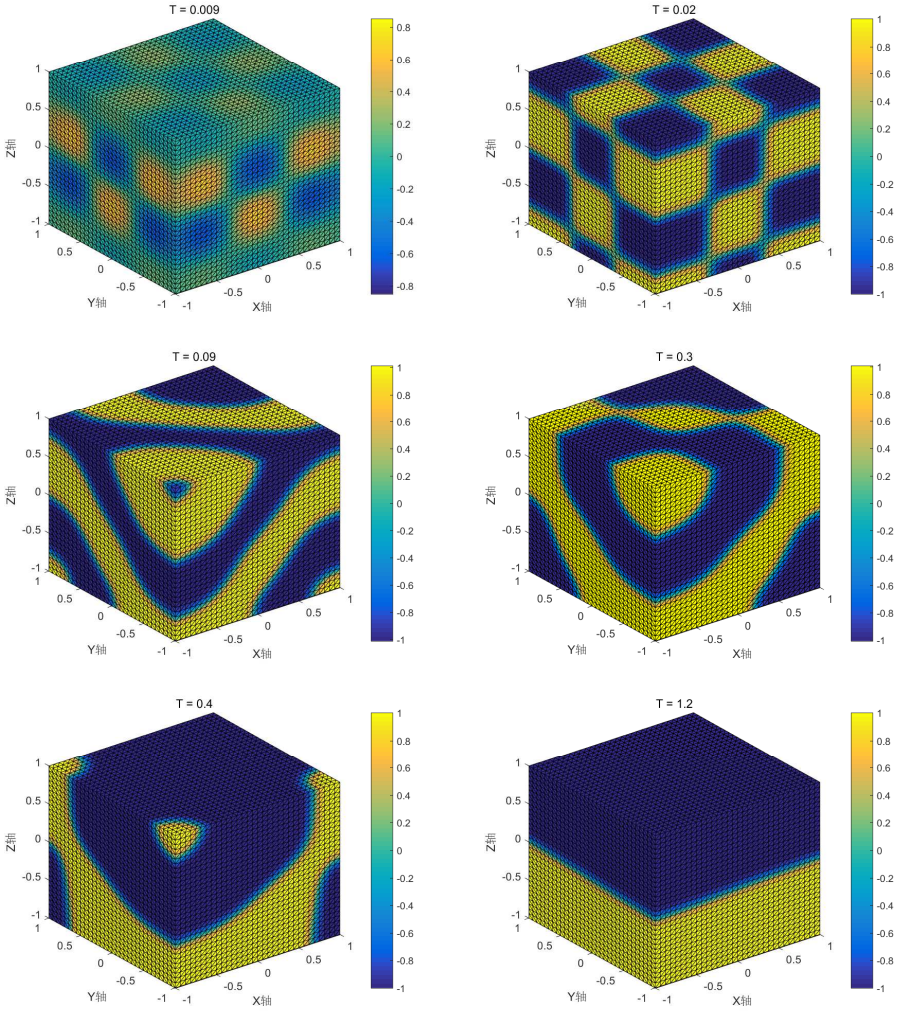

Figure 3: Example 4.3, h=0.1, τ=1.0e−04 and A=0.01, the numerical solutions at t=0.009,0.02,0.09,0.3,0.4,1.2.

to temporal discretization with a spatial mesh size $h=\frac{1}{200000}$. The corresponding numerical results at $T=1$ with different time step size are reported in Table 4. The numerical results evidently indicate a second order convergence rate in time.

Example 4.5. In this example, numerical simulations of the evolution of a initial data's interfaces are presented. We consider the Cahn-Hilliard equation (1.2) with $\epsilon=6.25e-05$. The initial value is given by

$$u_0(x_1,x_2)=\tanh\left(\frac{1}{\sqrt{2}\epsilon}\min\left\{\sqrt{(x_1+0.3)^2+x_2^2}-0.3,\sqrt{(x_2-0.3)^2+x_2^2}-0.25\right\}\right).$$

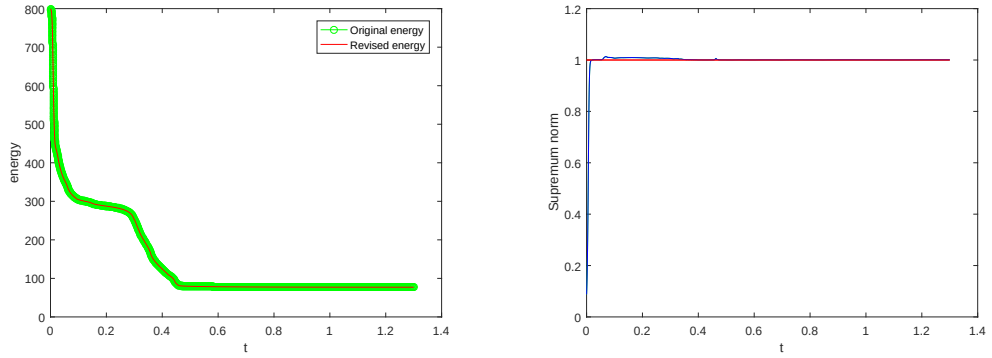

(a) (b)

Figure 4: Example 4.2. $h=0.1$, $\tau=1.0e-04$ and $A=0.01$, (a): time evolution of the original energy and revised energy; (b): time history of supremum norm.

Table 3: Example 4.4. Errors and convergence rate of the spatial discretization accuracy test for scheme (3.14), $\tau=10^{-6}$, $A=1.5$.

h	1/16	1/32	1/64	1/128	1/256
$\|u-u_h\|_{L^2}$	1.80e-03	4.43e-04	1.11e-04	2.77e-05	6.91e-06
order	-	2.02	2.00	2.00	2.00
$\|u-u_h\|_{H^1}$	1.14e-01	5.70e-02	2.85e-02	1.42e-02	7.1e-03
order	-	1.00	1.00	1.00	1.00

Table 4: Example 4.4. Errors and convergence rate of the temporal discretization accuracy test for scheme (3.14), $h=\frac{1}{200000}$, $A=1.5$.

τ	1/16	1/32	1/64	1/128	1/256
$\|u-u_h\|_{L^2}$	3.40e-3	8.48e-04	2.12e-04	5.30e-05	1.32e-05
order	-	2.00	2.00	2.00	2.00
$\|u-u_h\|_{H^1}$	1.76e-02	4.50e-03	1.10e-03	2.83e-04	7.08e-05
order	-	1.97	2.00	1.96	2.00

The computational domain $\Omega=(-1,1)\times(-1,1)$ is uniformly partitioned with a 128×128 cells and take the time step $\tau=0.0005$. From Fig. 5, it is observed that the initial interface that inclose two separated circles gradually evolves into one circle, which is consistent with the results reported in [16]. The time history of the discrete original energy is also plotted, which shows that the energy curve decreases with respect to time as the theory guaranteed.

Example 4.6. In this example, we consider the Eq. (1.2) in three dimensions. The initial value is a small random perturbation around zero:

$$u_0(x_1,x_2,x_3)=0.006rand(x_1,x_2,x_3)-0.003,$$

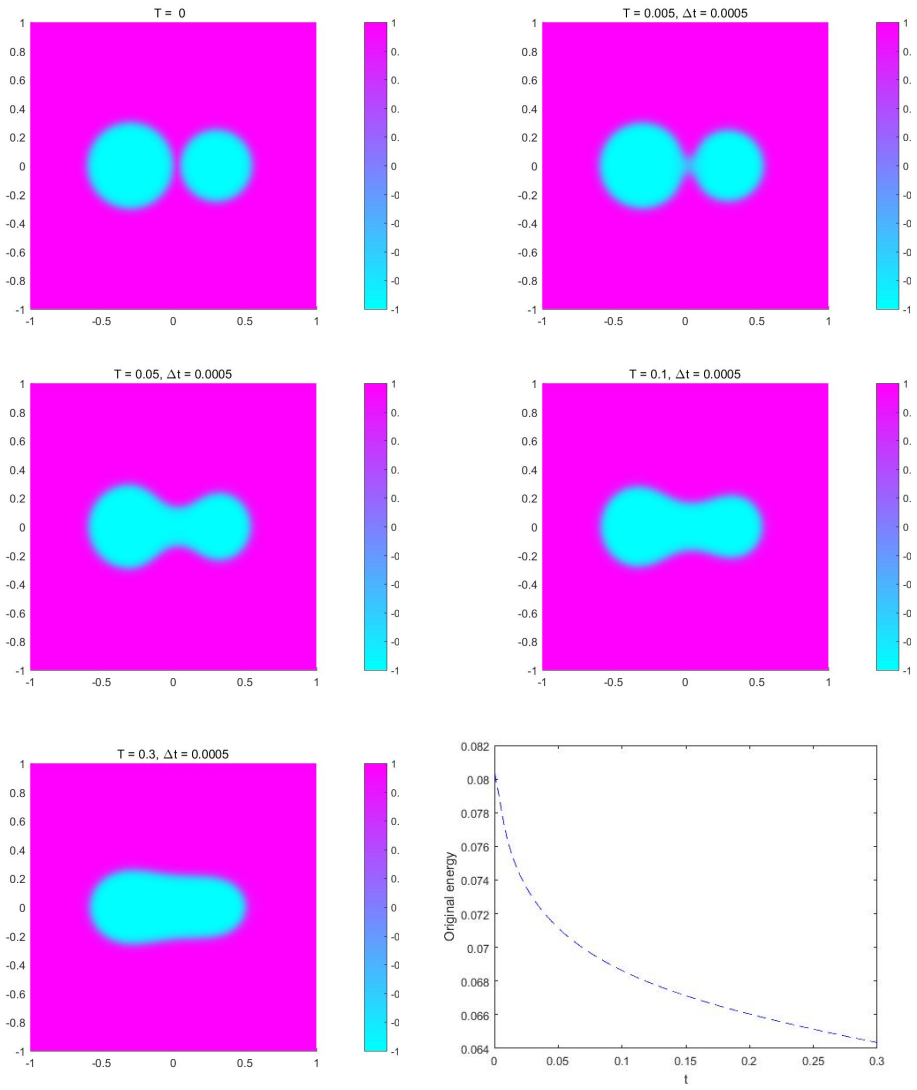

Figure 5: Example 4.5, $N=128$, $\tau=0.0005$, $A=2$, the evolution of the two-circle interface at five temporal frames and time evolution of the discrete original energy.

where $rand(\,)$ generates uniformly distributed random numbers on the unit interval. The solution domain is considered a cubic $\Omega=[-1,1]^3$, and $\epsilon=\sqrt{0.008}$.

Fig. 6 show the evolution solution of $u(x_1,x_2,x_3,t)$ at five different times, from which we can observe the solution tends to the steady state by increasing the time. From Fig. 6 we also found the original energy decays with respect to time.

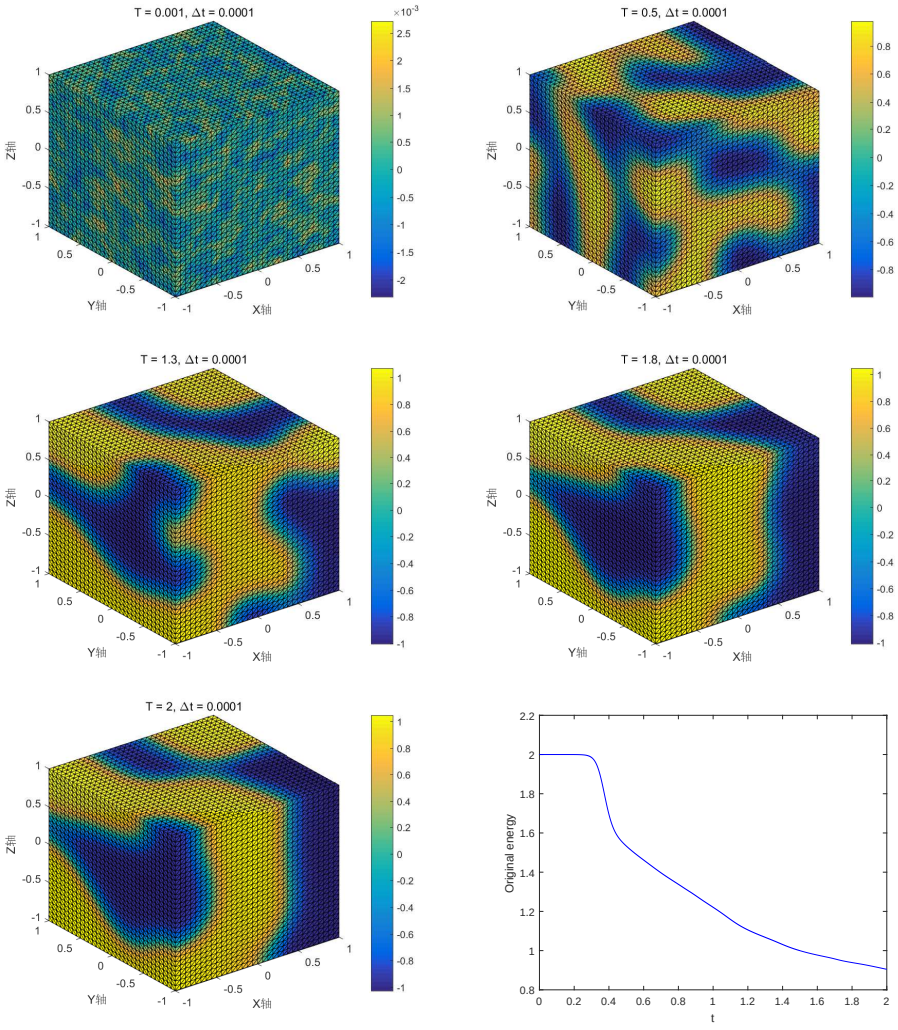

Figure 6: Example 4.6, $h=\frac{1}{10}$, $\tau=\frac{1}{10000}$ and $A=1000$, the evolution of $u(x,y,z,t)$ at five temporal frames and time evolution of the discrete original energy.

5 Conclusions

In this paper, we develop two unconditionally energy stable second-order numerical methods for solving the Allen-Cahn and Cahn-Hilliard equations. The finite element method is used for spatial discretization and semi-implicit schemes in which the linear term is treated implicitly and the nonlinear term is treated explicitly with a second order extrapolation, are used for temporal discretization. Comparing with classical semi-implicit methods, a single stabilizing term is introduced to ensure unconditional energy stability and a relatively large time step size could be utilized for a long time simula-

tion. Error estimates for the proposed numerical schemes are derived which show these two schemes are second order accurate in time discretization. Finally, several numerical examples were presented to verify the accuracy, efficiency and stability of the proposed schemes.

Acknowledgements

Li's research was supported by Department of Education of Hunan Province Project (No. 22C0491), Zhou's research was supported by key project of Hunan Education Department (No. 23A0143) and National Key Research and Development Program of China (No. 2023YFA1009100).

References

[1] S. M. ALLEN AND J. W. CAHN, *A microscopic theory for antiphase boundary motion and its application to antiphase domain coarsening,* Acta MeTall. Mater., 27 (1979), pp. 1085–1095.
[2] H. BREZIS, Functional Analysis, Sobolev Spaces and Partial Differential Equations, Springer, New York, 2010.
[3] J. BARRETT, J. BLOWEY, AND H. GARCKE, *Finite element approximation of the Cahn-Hilliard equation with degenerate mobility,* SIAM J. Numer. Anal., 37 (1999), pp. 286–318.
[4] X. CHEN, X. QIAN AND S. SONG, *Fourth-order structure-preserving method for the conservative Allen-Cahn equation,* Adv. Appl. Math. Mech., 15 (2023), pp. 159–181.
[5] L. Q. CHEN AND J. SHEN, *Applications of semi-implicit Fourier-spectral method to phase-field equations,* Comput. Phys. Commun., 108 (1998), pp. 147–158.
[6] C. COLLINS, J. SHEN AND S. M. WISE, *An efficient, energy stable scheme for the Cahn-Hilliard-Brinkman system,* Commun. Comput. Phys., 13 (2013), pp. 929–957.
[7] L. DEDÈ, H. GARCKE AND K. LAM, *A Hele-Shaw-Cahn-Hilliard model for incompressible two-phase flows with different densities,* J. Math. Fluid. Mech., 20 (2018), pp. 531–567.
[8] Q. DU AND R. A. NICOLAIDES, *Numerical analysis of a continuum model of phase transition,* SIAM J. Numer. Anal., 28 (1991), pp. 1310–1322.
[9] D. J. EYRE, *An unconditionally stable one-step scheme for gradient systems,* `http://www.math.utah.edu/eyer/research/methods/stable.ps`, 1998.
[10] D. J. EYRE, *Unconditionally gradient stable time marching the Cahn-Hilliard equation,* MRS Online Proceedings Library, `https://doi.org/10.1557/PROC-529-39`, Mater. Res. Soc. Sympos. Proc., 529 (1998), pp. 39–46.
[11] C. M. ELLIOTT AND A. M. STUART, *The global dynamics of discrete semilinear parabolic equations,* SIAM J. Numer. Anal., 30 (1993), pp. 1622–1663.
[12] D. FURIHATA, *A stable and conservative finite difference scheme for the Cahn-Hilliard equation,* Numer. Math., 87 (2001), pp. 675–699.
[13] X. B. FENG, *Fully discrete finite element approximations of the Navier-Stokes-Cahn-Hilliard diffuse interface model for two-phase fluid flows,* SIAM J. Numer. Anal., 44 (2006), pp. 1049–1072.
[14] X. B. FENG AND A. PROHL, *Numerical analysis of the Cahn-Hilliard equation and approximation for the Hele-Shaw problem,* Interfaces Free Bound., 7 (2005), pp. 1–28.
[15] X. B. FENG AND H. WU, *A posteriori error estimates and an adaptive finite element method for the Allen-Cahn equation and the mean curvature flow,* J. Sci. Comput., 24 (2005), pp.121–146.

[16] X. B. FENG, Y. LI, AND Y. XING, *Analysis of mixed interior penalty discontinuous Galerkin methods for the Cahn-Hilliard equation and the Hele-Shaw flow,* SIAM J. Numer. Anal., 54 (2016), pp. 825–847.
[17] X. L. FENG, T. TANG, AND J. YANG, *Stabilized Crank-Nicolson/ Adams-Bashforth schemes for phase field models,* Eeat Asian J. Appl. Math., 3 (2013), pp. 59–80.
[18] F. GUILLN-GONZLEZ AND G. TIERRA, *Second order schemes and time-step adaptivity for Allen-Cahn and Cahn-Hilliard models,* Comput. Math. Appl., 68 (2014), pp. 821–846.
[19] L. GOLUBOVIC, A. LEVANDOVSKY AND D. MOLDOVAN, *Interface dynamics and far-from-equilibrium phase transitions in multilayer epitaxial growth and erosion on crystal surfaces: Continuum theory insights,* East Asian J. Appl. Math., 1 (2011), pp. 297–371.
[20] S. GENG, T. LI, Q. YE AND X. YANG, *A new conservative Allen-Cahn type Ohta-Kawaski phase-field model for diblock copolymers and its numerical approximations,* Adv. Appl. Math. Mech., 14 (2022), pp. 101–124.
[21] Y. HE, Y. LIU AND T. TANG, *On large time-stepping methods for the Cahn-Hilliard equation,* Appl. Numer. Math., 57 (2007), pp. 616–628.
[22] J. CAHN AND J. HILLIARD, *Free energy of a non-uniform system I: interfacial free energy,* J. Chem. Phys., 28 (1958), pp. 258–267.
[23] L. HE AND Y. LIU, *A class of stable spectral methods for the Cahn-Hilliard equation,* J. Comput. Phys., 228 (2009), pp. 5101–5110.
[24] Z. HU, S. WISE, C. WANG AND J. LOWENGRUB, *Stable and efficient finite-difference nonlinear-multigrid schemes for the phase field crystal equation,* J. Comput. Phys., 228 (2009), pp. 5323–5339.
[25] D. KESSLER, R. H. NOCHETTO AND A. SCHMIDT, *A posteriori error control for the Allen-Cahn problem: circumventing Gronwall's inequality,* ESAIM: Math. Model. Numer. Anal., 38 (2004), pp. 129–142.
[26] J. KIM, *Phase-field models for multi-component fluid flows,* Commun. Comput. Phys., 12 (2012), pp. 613–661.
[27] T. OHTA AND K. KAWASAKI, *Equilibrium morphology of block copolymer melts,* Macromolecules, 19 (1986), pp. 2621–2632.
[28] C. LI, Y. HUANG AND N. YI, *An unconditionally energy stable second order finite element method for solving the Allen-Cahn equation,* J. Comput. Appl. Math., 353 (2019), pp. 38–48.
[29] D. LI AND Z. QIAO, *On second order semi-implicit Fourier spectral methods for 2d Cahn-Hilliard equations,* J. Sci. Comput., 70 (2017), pp. 301–341.
[30] I. OHNISHI, Y. NISHIURA, AND M. IMAI, ET AL., *Analytical solutions describing the phase separation driven by a free energy functional containing a long-range interaction term,* Chaos, 9 (1999), pp. 329–341.
[31] Z. QIAO AND Q. ZHANG, *Two-phase image segmentation by the Allen-Cahn equation and a nonlocal edge detection operator*, Numer. Math. Theor. Meth. Appl., 15 (2022), pp. 1147–1172.
[32] J. SHEN, J. XU AND J. YANG, *The scalar auxiliary variable (SAV) approach for gradient flows,* J. Comput. Phys., 353 (2018), pp. 407–416.
[33] J. SHEN, J. XU AND J. YANG, *A new class of efficient and robust energy stable schemes for gradient flows,* SIAM Rev., 61 (2019), pp. 474–506.
[34] J. SHEN AND X. YANG, *Numerical approximations of Allen-Cahn and Cahn-Hilliard equations,* Disc. Contin. Dyn. Syst., 28 (2010), pp. 1669–1691.
[35] N. TAKADA, M. MISAWA AND A. TOMIYAMA, *A phase-field method for interface-tracking simulation of two-phase flows,* Math. Comput. Simul., 72 (2006), pp. 220–226.
[36] V. THOMÉE, Galerkin Finite Element Methods for Parabolic Problems, Springer, Second Edi-

tion, 2006.
[37] S. WISE, C. WANG AND J. LOWENGRUB, *An energy-stable and convergent finite-difference scheme for the phase field crystal equation,* SIAM J. Numer. Anal., 47 (2009), pp. 2269–2288.
[38] C. XU AND T. TANG, *Stability analysis of large time-stepping methods for epitaxial growth models,* SIAM J. Numer. Anal., 44 (2006), pp. 1759–1779.
[39] Y. XIA, Y. XU AND C.-W. SHU, *Application of the local discontinuous galerkin method for the Allen-Cahn/ Cahn-Hilliard system,* Commun. Comput. Phys., 5 (2008), pp. 821–835.
[40] M. YUAN, W. CHEN, C. WANG, S. M. WISE AND Z. ZHANG, *A second order accurate in time, energy stable finite element scheme for the Flory-Huggins-Cahn-Hilliard equation,* Adv. Appl. Math. Mech., 14 (2022), pp. 1477–1508.
[41] YIN YANG, JIANYONG TAO, SHANGYOU ZHANG, PETR V. SIVTSEV, *A Jacobi collocation method for the fractional Ginzburg-Landau differential equation,* Adv. Appl. Math. Mech., 12 (2020), pp. 57–86.
[42] X. YANG, *Linear, first and second-order, unconditionally energy stable numerical schemes for the phase field model of homopolymer blends,* J. Comput. Phys., 327 (2016), pp. 294–316.
[43] X. YANG AND L. JU, *Efficient linear schemes with unconditional energy stability for the phase field elastic bending energy model,* Comput. Methods Appl. Mech. Eng., 315 (2017), pp. 691–712.
[44] X. YANG AND L. JU, *Linear and unconditionally energy stable schemes for the binary fluid-surfactant phase field model,* Comput. Methods Appl. Mech. Eng., 318 (2017), pp. 1005–1029.
[45] X. YANG, J. ZHAO AND Q. WANG, *Numerical approximations for the molecular beam epitaxial growth model based on the invariant energy quadratization method,* J. Comput. Phys., 333 (2017), pp. 104–127.
[46] H. YU AND X. YANG, *Numerical approximations for a phase-field moving contact line model with variable densities and viscosities,* J. Comput. Phys., 334 (2017), pp. 665–686.
[47] X. YANG, J. ZHAO, Q. WANG AND J. SHEN, *Numerical approximations for a three components Cahn-Hilliard phase-field model based on the invariant energy quadratization method,* Math. Models Methods Appl. Sci., 27 (2017), pp. 1–38.
[48] S. ZHANG AND M. WANG, *A nonconforming finite element method for the Cahn-Hilliard equation,* J. Comput. Phys., 229 (2010), pp. 7361–7372.